Frequency and hold time influence on crack growth behavior of a 9 - 12 % Cr ferritic martensitic steel at temperatures from 300 °C to 600 °C in air.

T. Fischer, B. Kuhn

Forschungszentrum Juelich GmbH, Institute for Energy and Climate Research (IEK), Microstructure and Properties of Materials (IEK-2), Juelich, Germany

Abstract

Due to an increase of renewable energies proportion, e. g. wind power and photovoltaics, which cannot supply energy constantly, modern power plants must be able to be operated flexibly in order to compensate the residual load. As a consequence of increasing alternating load, fatigue damage becomes more and more important, while creep damage caused by ever shorter holding times at high operating temperature decreases. In this study a turbine bypass valve, one of the most fatigue loaded power plant component, manufactured from widespread standard 12 % Cr ferritic/martensitic steel X20 was investigated. Fatigue crack growth experiments showed that the crack growth rate increases slightly with decreasing frequency (20 Hz → 5 Hz). In hold time tests (300 s → 600 s, effective frequency 3.33×10^{-3} Hz → 8.33×10^{-4}), larger crack propagation rates per cycle occur than in the fatigue crack growth experiments with 5 and 20 Hz. In comparison to pure cyclic loading maximum load holding time further required significantly higher ΔK values to start crack growth.

Keywords: Fatigue, Creep-Fatigue, Crack growth, Frequency, Hold time, 9 - 12 % Cr steels

1. Introduction

Recently the requirements for conventional power plants changed fundamentally: Modern power plants must be capable of flexible operation (frequent start-ups and shut-downs, load following operation) to compensate for power requirements caused by fluctuating renewable sources of energy, what causes by far greater temperature and pressure fluctuations during operation. For this reason the applied materials face by far more demanding loading scenarios than in the past. As a consequence of increased cyclic operation fatigue damage becomes more dominant, whereas diminishing base load operation decreases the importance of creep damage.

In this respect thick-section components of the feed water and live steam systems, e. g. spheroidal forgings, fittings, collectors, pumps and turbine bypass valves (TBV) are of particular importance. In the current study material from two ex-service TBVs (operation duration ~ 21 years) was investigated. The TBV was chosen because it is subjected to the most demanding cyclic loading profile during plant start-up and shut-down and thus represents the most fatigued component. Technically, the TBV is a separation between the steam systems of differing pressure. The TBV was manufactured from German X20CrMoV12-1 grade, a tempered 12 % Cr ferritic-martensitic steel largely used especially in the German power industry [1, 2].

The aim of the study, carried out in the framework of the joint national “THERRI” (German: THermisches ERmüdungsRIsswachstum, engl.: Thermal fatigue crack propagation; grant number: 03ET7024A) project under funding of the German Federal Ministry of Economic

Affairs and Energy, was to characterize the crack propagation behavior of X20CrMoV12-1 depending on the cycling frequency in the temperature range from 300 °C to 600 °C, which is relevant for flexibly operated power plants. Within the THERRI project the experimental results served as part of the data basis for the elaboration of an improved code for remaining life assessment by identification of cyclic lifetime reserves of the material, which are not properly exploited by existing codes.

Numerous studies [3-10] have discussed the fundamental influence of temperature on fatigue crack growth. Generally the rate of crack growth increases with temperature at a given amplitude of stress intensity. The crack growth behavior of engineering alloys under creep-fatigue conditions has also been investigated in several studies [11-19].

The influence of maximum load holding times in the temperature range from 600 °C to 625 °C on fatigue crack propagation in 9 - 12 % Cr steels was investigated in [15, 16, 18, 20]. Contrary to that, only limited or no crack propagation data are available for X20CrMoV12-1 steel in the temperature range from 300 °C to 600 °C, which is most relevant for flexibly operated power plants. Furthermore the potentially significant effect of cycling frequency for better utilization of material inherent strength potentials is not properly reflected in literature. The present study is intended to provide the basis to overcome this lack of knowledge.

For the high temperature range from 600 °C to 625 °C the following relationships are known. An increase in holding time caused accelerated cyclic crack growth. Nikbin et al. [21] investigated the martensitic steel FV448 at 550 °C applying so-called compact tension (CT) (specimen geometry outlined in [21]) specimens at a constant load ratio of R = 0.1 at frequencies between 10^{-3} and 10 Hz. At frequencies less than 0.01 Hz the investigated creep crack failure mode conformed to static creep crack growth tests, whereas an interaction region was found in the frequency range from 1 to 0.01 Hz. Narasimhachary et. al. [15] investigated P91 steel at 625 °C under constant load amplitude conditions with various holding times using compact tension specimens and showed that the crack growth rates increased significantly with increase in holding time, when the crack growth rates per cycle were plotted against cyclic stress intensity factor ΔK. Bassi et al. [16] performed creep fatigue tests on T/P91 steel at 600 °C on standard CT specimens. For creep-fatigue loading conditions (holding times of 0.1 h) pure fatigue crack growth was evident, while for holding times between 1 and 10 h pure creep crack growth was confirmed. Between 0.1 and 1 h a transition from cycle to time dependent crack growth behavior was thus anticipated. Shi et. al. [18] investigated the creep and creep fatigue crack growth behavior of P92 steel at 600 °C. The results showed that crack growth behavior is dominated by the cycle-dependent fatigue process at shorter holding times and turns to be dominated by the time-dependent creep process when the holding times become longer.

2. Material and Methods

The current study focused on ex-service material taken from a turbine bypass valve (fabricated by Bopp & Reuther) taken out of service after ~ 21 years of operation in a coal-fired power plant operated by KNG Rostock, KNG: Kraftwerks- und Netzgesellschaft mbH, **Figure 1**).

Figure 1: Turbine bypass valve (fabricator: Bopp & Reuther).

The TBV body has been produced by open-die forging of X20CrMoV12-1. The chemical specification of the material is given in Table 1.

Table 1: Chemical composition of X20CrMo V12-1 to standard DIN 17175 (in wt %):

	C	Si	Mn	P	S	Cr	Mo	Ni	V
X20CrMo V12-1	0.17	≤0.50	≤1.00	≤0.030	≤0.030	10.00	0.80	0.30	0.25
	0.23					12.50	1.20	0.80	0.35

A modified (due to TBV dimensions) compact tension (CT) specimen geometry with a width, W = 40 mm and thickness, B = 10 mm and an initial notch, a_0 = 10 mm was chosen for the experimental program. The dimensions chosen were in accordance with ASTM test standard [25]. The specimens were taken from the "cold flange", which had not been in contact with steam after dismantling the TBV (**Figure 2)**.

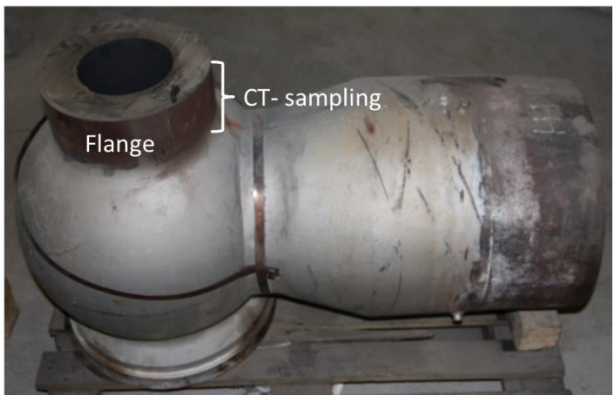

Figure 2: CT- sampling from the dismantled TBV: Specimens were taken from the "cold flange", which that had not been in contact with steam.

The "cold flange" material was chosen because no microstructural degradation was expected from operation and it was intended to start with a basic study of the material in virgin condition. The virgin condition of the material for this reason was verified by examination of the tensile properties, which did not show significant deviation from the specified (**Table 2**). Additional EBSD-analysis prove the expected martensite lath microstructure (**Figure 3**) being completely preserved.

Table 2: Tensile properties of X20CrMoV12-1 steel at temperatures from ambient (RT) up to 600 °C in comparison to values read off the graphs in the X20 data sheets *[22] (for this reason the values are denoted as approximate values), taken from the **standard DIN 17175 and *[23].**

Temperature [°C]	σ_{UTS} [MPa]	σ_{UTS}* [MPa]	σ_{UTS}** [MPa]	σ_{YS} [MPa]	Y [GPa]	Y*** [GPa]	A [%]	Ag [%]
RT	777.12	~760	650-850	587.16	210	218	17.25	8.2
300	645.88	~560	-	490.45	190	198	13.55	7.1
400	594.07	~510	-	445.55	182	189	12.15	5.5
500	487.00	~400	-	393.74	172	179	19.95	3.9
550	411.01	~330	-	338.48	167	-	23.95	2.8
600	324.67	-	-	245.23	160	166	37.55	1.6

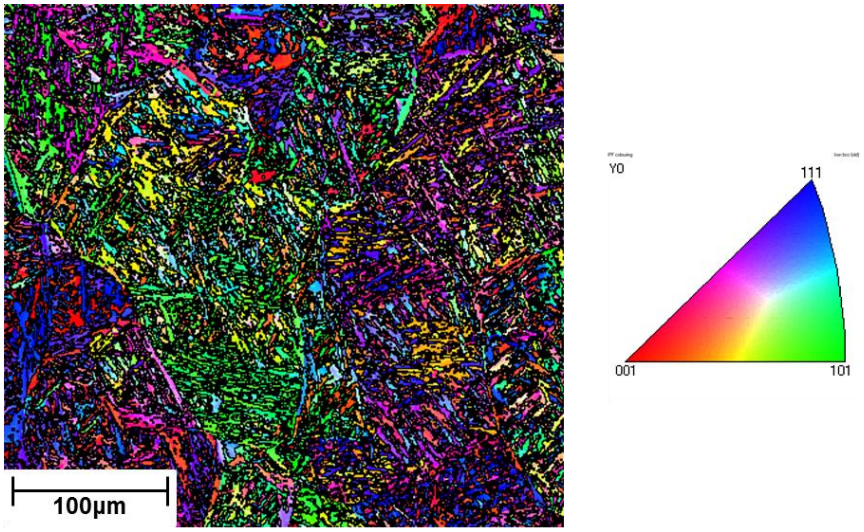

Figure 3: EBSD-orientation map taken from the"cold flange" of the TBV, which had not been in contact with hot steam, reflecting no changes in microstructure.

Fatigue tests were performed applying a sinusoidal wave form at a constant force. **Figure 4** displays the cyclic loading schedule applied in the holding time tests. Loading was accomplished within 1 s from minimum to maximum load, the maximum load was then held constant between 300 s and 1200 s, followed by load removal corresponding to the load ratio R (again within 1 s). The minimum load is then held constant for 1s before the cycle starts over again until the termination criterion is reached (either a/W = 0.7 or 5 mm extension).

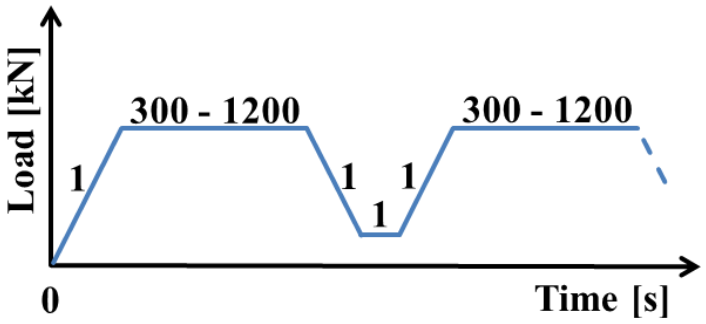

Figure 4: **Cyclic loading scheduled executed in case of the hold time tests.**

Fatigue crack growth (FCG) testing was conducted in a servo hydraulic testing machine (Instron Model 1343). Hold time experiments were executed in an electromechanical testing machine (Instron Model 1362). In both set-ups the specimens were inductively heated. Before testing the CT specimens were pre-cracked to a starter crack length to width ratio (a/W) of about 0.4 by cyclic loading at ambient temperature in an Instron Model 1603 resonance tester. The direct current potential drop (PD) technique was used to continuously monitor the crack length, employing a linear calibration.

The cyclic stress intensity factor ΔK for the CT specimen was determined according to ASTM [24]. The calculation of the cyclic crack growth rate was accomplished by a 7-point polynomial method according to ASTM [24]. All the tests were carried out in a temperature range from 300 °C to 600 °C, applying an R value of 0.1 in laboratory air. The FCG tests were conducted at 5 and 20 Hz. In the hold time experiments, the holding time was varied from 300 s up to 1200 s.

After the experiment the fracture surfaces were cut from the CT specimen and measured excluding the pre-crack and residual fracture surface. Furthermore all the fracture surfaces were observed for microstructure at longitudinal sections. For this purpose the fracture surfaces were hot embedded for metallographic preparation, grounded, polished and electrolytically etched with H_2SO_4. Microstructural investigation was performed utilizing a Zeiss Merlin field emission scanning electron microscope (FESEM). Additionally the specimens were polished for 2-3 h to a sub-micron finish in colloidal silica suspension for electron backscatter diffraction (EBSD) analysis, which was carried out at a Zeiss Merlin SEM equipped with Oxford Instruments EBSD-(NORD LYS 2 camera) and EDX- (X Max 150) systems.

3. Results and Discussion

Near threshold behavior was excluded, because the effects of temperature and frequency on stable crack growth (within the so called “Paris-Erdogan regime”, cf. [25]) were in the focus of this study. The colored solid lines in **Figure 5** represent the fitted lines of the stable crack growth ranges of the fatigue crack growth (FCG) experiments with 20 Hz in the temperature range from 300 °C to 600 °C in air applying the Paris equation (also shown in **Figure 5**) [25]. The associated fatigue crack growth parameters are listed in **Table 3**.

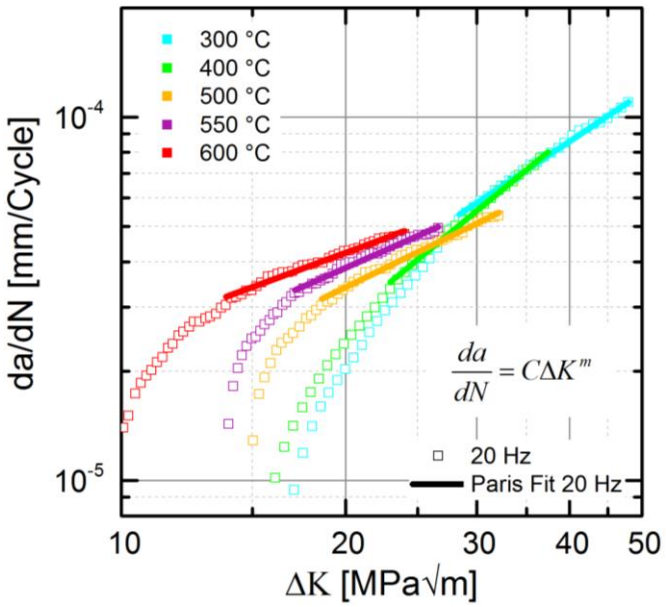

Figure 5: **Fatigue crack growth behavior of X20CrMoV12-1 at f = 20 Hz, R = 0.1, T: 300 °C - 600 °C, corresponding Paris fit-curves for each individual temperature.**

At corresponding stress intensity the crack growth rate increased slightly as a function of temperature. With increasing temperature the test termination criterion (a / W = 0.7) is achieved at lower stress intensity. Consequently, a component will fail at lower stress intensity. The coefficient C increased by about one order of magnitude in the range from 400 °C to 500 °C and then remained merely unchanged up to 600 °C. The exponent m increased slightly up to 400 °C, then decreased in the range from 400 °C to 500 °C and remained almost constant up to 600 °C. A decreasing trend of m with increasing temperature became evident.

In order to investigate the effect of lower testing frequency, FCG-experiments were performed at 5 Hz (**Figure 6**). Like in the case of the 20 Hz FCG tests the stable crack growth range was fitted in the whole temperature range from 300 °C to 600 °C using the Paris equation (dotted colored lines in **Figure 6**) and the associated fatigue crack growth parameters are listed in **Table 4**. In comparison to 300 °C the crack growth rate at 400 °C was marginally lower at corresponding stress intensities. From 400 °C to 500 °C a rise / drop in coefficient C / m became obvious, while starting from 500 °C both coefficients remained merely unchanged towards higher temperature.

Table 3: **Fatigue crack growth parameters, f = 20 Hz, air.**

Temperature [°C]	Coefficient C	Exponent m
300	5.70×10^{-7}	1.4
400	1.77×10^{-7}	1.7
500	1.72×10^{-6}	1.0
550	2.56×10^{-6}	0.9
600	4.41×10^{-6}	0.8

With temperature increasing from 400 °C the test termination criterion was achieved at lower stress intensity (**Figure 6**).

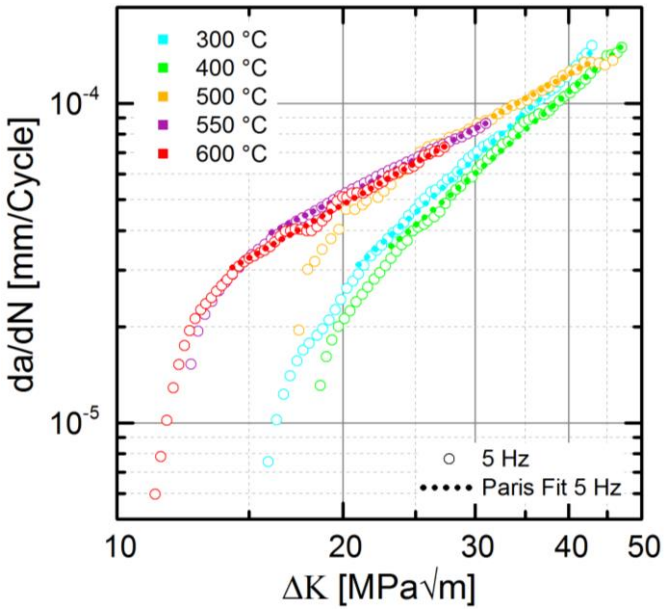

Figure 6: **Fatigue crack growth behavior of X20CrMoV12-1 at f = 5 Hz, R = 0.1, T: 300 °C - 600 °C, corresponding Paris fit-curves for each individual temperature.**

Table 4: **Fatigue crack growth parameters, f = 5 Hz, air.**

Temperature [°C]	Coefficient C	Exponent m
300	4.53×10^{-8}	2.1
400	5.90×10^{-8}	2.0
500	9.95×10^{-7}	1.3
550	1.43×10^{-6}	1.2
600	8.70×10^{-7}	1.3

Figure 7 displays the Paris fit-curves of the cyclic crack growth curves of the FCG tests at both testing frequencies in the temperature range from 300 °C to 600 °C. The crack growth rate increases slightly with decreasing frequency (20 Hz → 5 Hz) in the entire temperature range from 300 °C to 600 °C.

Over the entire temperature range the fatigue crack growth parameter C was approximately one order of magnitude higher at 20 Hz than at 5 Hz. In contrast, the exponent m was lower in the entire temperature range.

In order to test the effect of very low frequency loading, like it occurs in real power plant operation, FCG tests were carried out with 300 s of holding time at maximum load. The

maximum allowable operating temperature of X20CrMoV12-1 steel is 550 °C. Nevertheless experiments were carried out up to 600 °C to characterize the effect of overheating events caused by off-standard operating conditions. The transition from fatigue-dominated crack

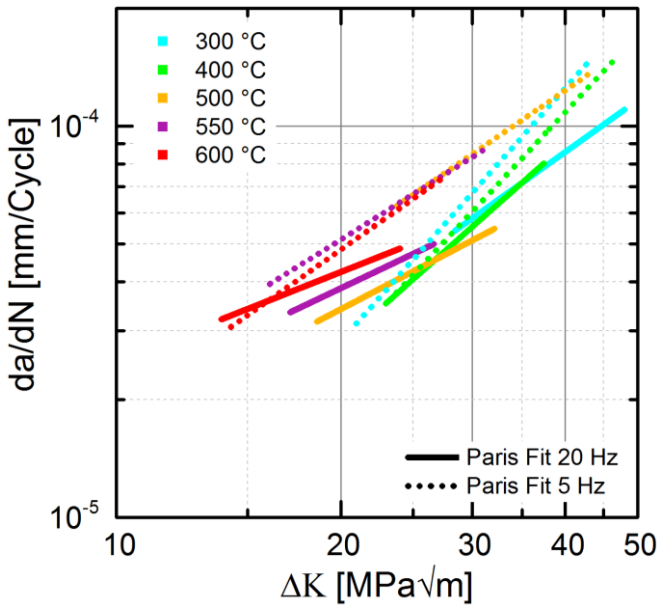

Figure 7: **Frequency influence (X20CrMoV12-1) on the crack growth rate at frequencies of 5 Hz and 20 Hz, R = 0.1, T: 300 °C - 600 °C.**

growth to creep-fatigue interaction is determined by the temperature / frequency / hold time combination, but was not in the focus of this study. In order to enable straight forward comparison of the crack growth curves measured from low up to high frequencies the evaluation of the hold time experiments was carried out according to the K-concept [26]. Determination of the transition from fatigue to creep-fatigue dominated damage and a more sophisticated evaluation concept (e. g. J-Integral [27, 28] or C*-Integral [29]) is in the focus of current and future work. **Figure 8** shows the cyclic crack growth curves of 300 s hold time tests at maximum load in the temperature range from 300 °C to 600 °C.

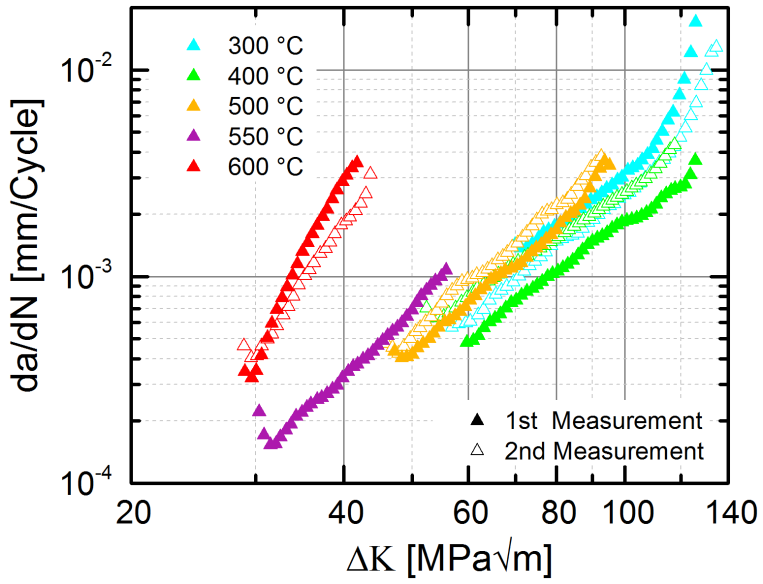

Figure 8: **Crack growth behavior of X20CrMoV12-1 in 300 s hold time at maximum load experiments, R = 0.1, T: 300 °C - 600 °C.**

In the temperature range from 300 °C to 500 °C, the cyclic crack growth curves were found to be relatively close together (**Figure 8**), which in turn means that in this range there is only a weaker temperature dependency. At 550 °C a significant temperature influence was observed. Crack growth starts at significantly lower ΔK values and the test termination criterion (a/W = 0.7 or 5 mm extension) was reached at lower stress intensity (**Figure 8**). At 600 °C the crack growth rate was significantly increased (**Figure 8**). As a further step towards more realistic loading conditions experiments with 600 s holding time were conducted. Additionally another test with 1200 s hold time was carried out to identify the transition from fatigue-dominated crack growth to creep fatigue interaction. **Figure 9** displays a synopsis of the gathered results.

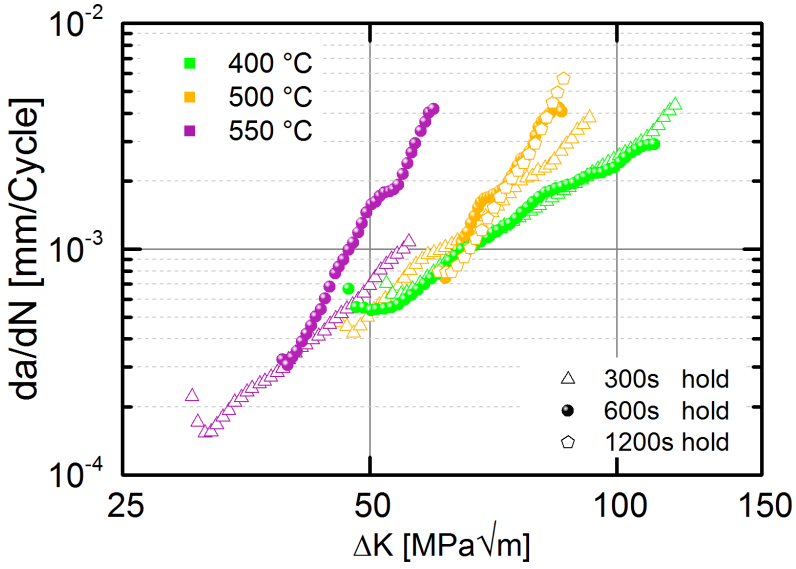

Figure 9: **Hold time influence on crack growth behavior (300 s, 600 s and 1200 s hold time at maximum load, R = 0.1, T: 400 °C - 550 °C).**

At 500 °C and 550 °C the crack growth rate increased with increasing holding time (**Figure 9**), what indicates creep. At 500 °C an increase in holding time beyond 600 s did not lead to a further increase in crack growth rate. In contrast the crack growth rate did not exhibit hold time sensitivity at 400 °C (cf. 600 s and 300 s hold time tests in **Figure 9**).

When a hold time is inserted into the testing cycles of creep-ductile materials (such as X20CrMoV12-1), the cyclic crack growth curve in the initial region often exhibits a hook-shaped pattern (cf. **Figure 9** and more detailed in **Figure 10**). The shape of the "hook" tends to decrease with decreasing temperature and increasing hold time. Saxena [20] found this "hook" in case of a Cr-Mo-V creep ductile steel at 538 °C with a hold time of 60 s at maximum load, Narasimhachary et. al. [15] at different hold times of up to 600 s, at R = 0.1 in 9Cr-1Mo (P91) steel at 625 °C. Narasimhachary et. al. [15] explained the "hook" by a combination of stress relaxation at the crack tip and an increase in the apparent crack length. In the beginning creep-deformation is considered to occur rapidly as a result of high elastic stresses. With accumulated time, creep deformation decelerates because at crack tip stresses relax as a consequence of redistribution. Furthermore, the rate of stress relaxation decreases with time, but at the same time ΔK increases due to the increasing crack length. These competing forces result in a tendency for the crack growth rate to first decrease and after passing a minimum to increase, what results in the "hook shape" in the da/dN vs. ΔK plot.

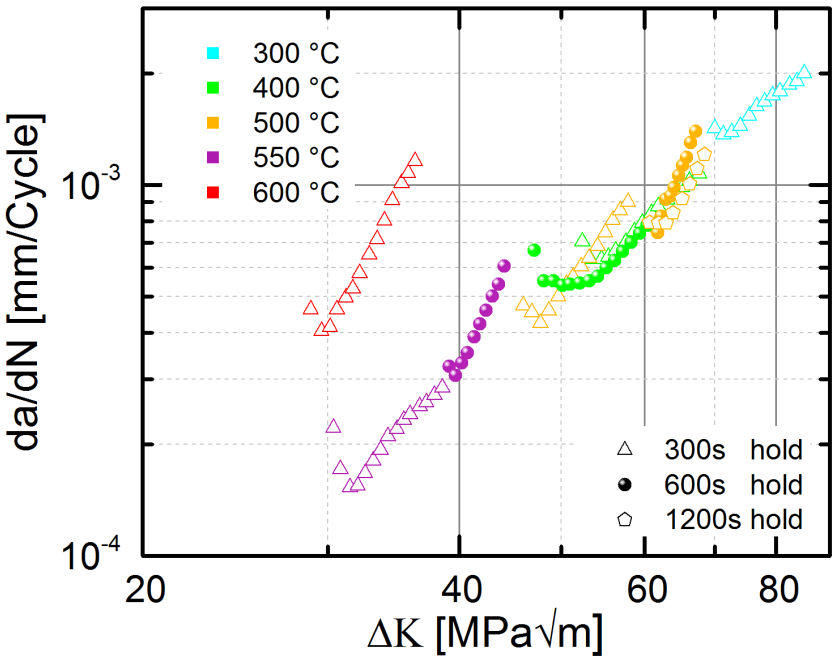

Figure 10: **Crack growth of creep ductile X20CrMoV12-1 (300 s, 600 s and 1200 s hold time at maximum load, R = 0.1, T: 300 °C - 600 °C).**

The investigations of Saxena [20] and Narasimhachary et. al. [15] were performed at temperatures above 500 °C. In this study, hold time tests were carried out in the temperature range from 300 °C to 600 °C. A trend towards hook formation is also observed in a less pronounced shape even at lower temperatures (**Figure 10**), where creep deformation does not occur. In comparison to elevated temperature high stress intensity is required at low temperature, to initiate crack growth (**Figure 10**). This results in a larger plastic zone in front

of the crack tip; consequently the crack growth rate decreases. Furthermore the crack growth rate decreases until the crack has grown sufficiently and ΔK has increased, so that the plastic zone in front of the crack tip can be overcome relatively simple. As a result the crack growth rate increases with rising ΔK. A possible explanation for the less pronounced “hook” at lower temperature could be that the crack growth rate is higher in the initial range of cyclic crack growth due to the required stress intensity at the onset of crack growth, despite high dislocation density and a large plastic zone in front of the crack tip (at the same hold time, **Figure 10**). Because of the higher crack growth rate, a ΔK value is reached faster, from which the high dislocation density and the large plastic zone can be easily overcome. Furthermore, it is observed that with increasing hold time, the "hooks" are less pronounced. This might be an indicator for pronounced stress relaxation during increased hold time.

Figure 11 displays the frequency dependence of the crack growth rate at R = 0.1 in a temperature range from 300 °C to 600 °C.

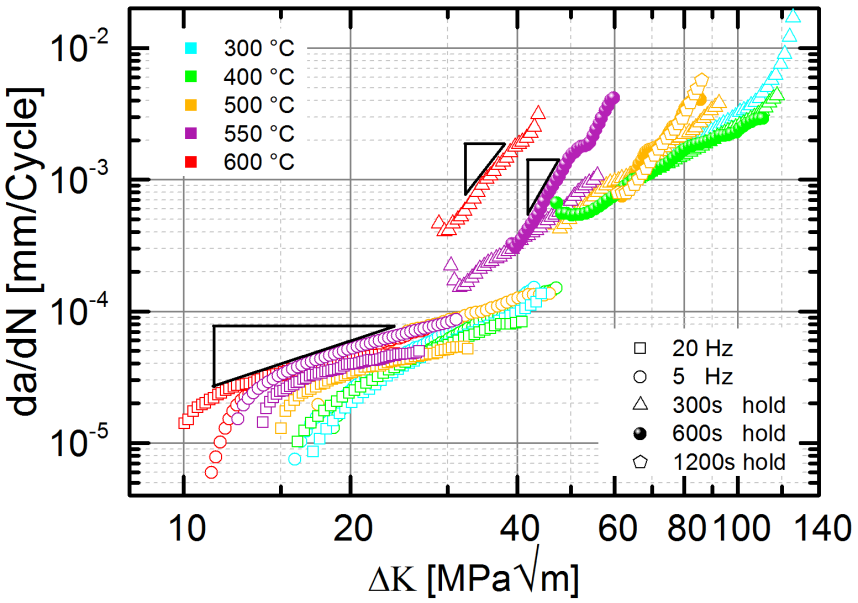

Figure 11: **Frequency influence at R = 0.1 on the crack growth rate and the start of crack growth, T: 300 °C - 600 °C.**

At given value of R and at high frequencies (5 Hz and 20 Hz) the crack growth rate increased slightly with decreasing frequency over the entire temperature range (**Figure 11**), i. e. the crack growth rate is relatively insensitive to testing frequency. At very low frequencies (starting from 300 s hold time) the crack growth rate increased significantly (**Figure 11**), what implies time-dependent effects. Nikbin et. al. [21] observed similar behavior at R = 0.1 for FV448 steel at 550 °C. Furthermore, significantly higher ΔK values are required in the hold time test in the entire temperature range for crack propagation (**Figure 11** and **Figure 12,** exemplary by comparing the hold time test with the FCG tests at 20 Hz).

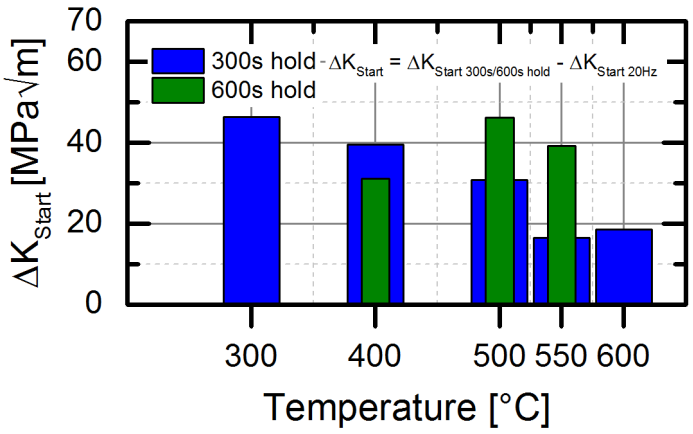

Figure 12: **Rise of the crack growth start value (ΔK_{Start}) in the 300 s and 600 s hold time experiments at maximum load, R = 0.1 (comparison of mean values, exception: 550 °C) in comparison to the 20 Hz FCG tests as a function of the temperature.**

Evaluation of the 300 s hold time test (**Figure 8**) uncovered conspicuous behavior: In comparison to all the temperatures the crack growth rate increased faster at even lower ΔK values at 600 °C only, what resulted in the question whether this was caused by pronounced creep or another mechanism. In order to clarify this the crack growth rates of all the 300 s hold time experiments were plotted over crack length at maximum load (**Figure 13a**).

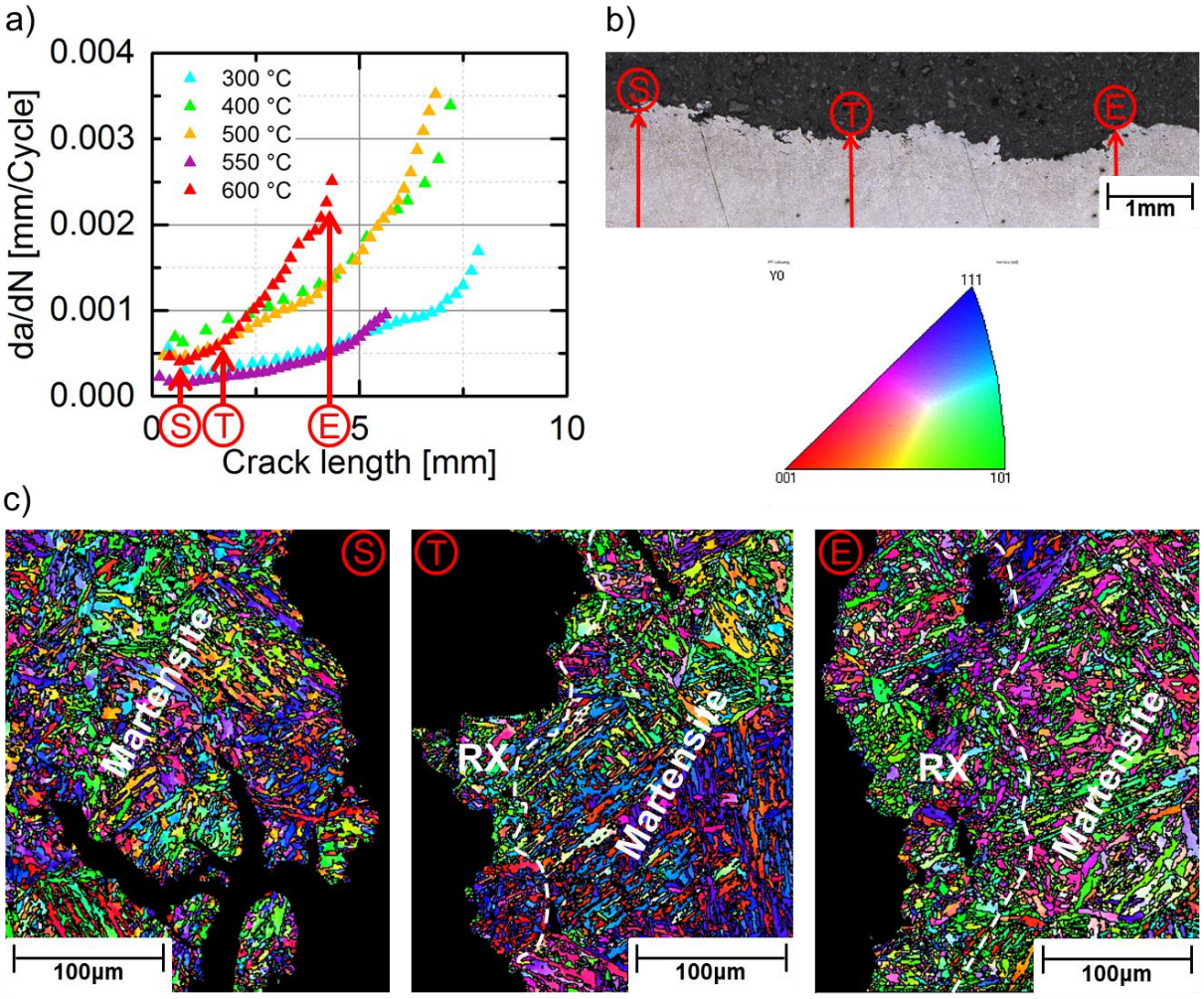

Figure 13: **a) Crack growth rate over crack length (300 s hold time experiments, T: 300 °C - 600 °C), b) positions of EBSD mappings performed at longitudinal sections of the crack edge of the 600 °C specimen and c) EBSD mappings (in crack propagation direction) at positions "S", "T" and "E" (cf. corresponding crack length values in Fig. 12a).**

In contrast to the lower temperatures the crack growth rate accelerates even at considerably lower crack length (~ 1.85 mm) at 600 °C. For this reason, EBSD crystal orientation mappings were carried out at position "S", where crack growth was initiated, at position "T", from which accelerated crack growth occurred and at position “E”, i. e. close to the end of the crack (cf. **Figure 13a, b**). The martensitic structure was completely retained in the crack initiation region (cf. **Figure 13c**: “S”), while recrystallization occurred from exactly the position at which accelerated crack growth occurred (cf. **Figure 13c:** "T"). Since recrystallization involves a decrease in dislocation density and results in a reduction of material strength it is supposed to be the reason for accelerated crack growth at 600 °C. A critical ΔK value for recrystallization of ~ 32 MPa√m and a crack rate of ~ 6.5×10^{-4} mm/cycle can be assigned to position "T" (by considering the measured crack length). In the crack end region (cf. **Figure 13c:** "E") the martensitic structure has completely disappeared close to the crack edges (cf. the martensitic structure in the virgin condition, depticted in Figure 3) while remaining intact at a greater distance from the crack edge. The reason for the stronger recrystallization towards the end of the crack is dynamic recrystallization, caused by high stress intensity. Therefore the remaining service life has to be calculated with the strength of the recrystallized structure from this up to higher stress intensities and not with the strength of

the martensite in case the of 600 °C hold time tests. **Figure 14** displays the cyclic crack growth curve of the FCG experiment at 5 Hz and the 300 s hold time test at 600 °C. The arrow indicates the beginning of recrystallization in the 300 s hold time experiment. It can easily be recognized that the deformation rates and stress intensities required for recrystallization were not achieved in the FCG test and for this reason recrystallization did not occur.

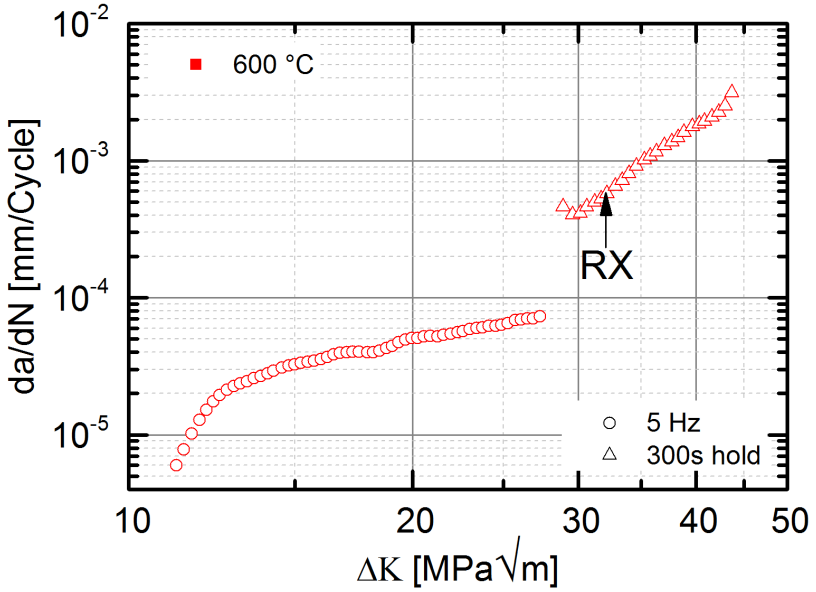

Figure 14: **Cyclic crack growth curve of the 5 Hz FCG test) and the 300 s hold time test at maximum load (T: 600 °C). Beginning of recrystallization marked by an arrow.**

For verification an EBSD mapping was taken near to the crack end region (highest stress intensity and crack growth rate) of the 5 Hz FCG test specimen. The martensitic structure was found to be completely retained at the edges of the crack end (**Figure 15**) with the martensite structure corresponding to the virgin condition (cf. Figure 3), what illustrates that recrystallization did not occur in the FCG experiment.

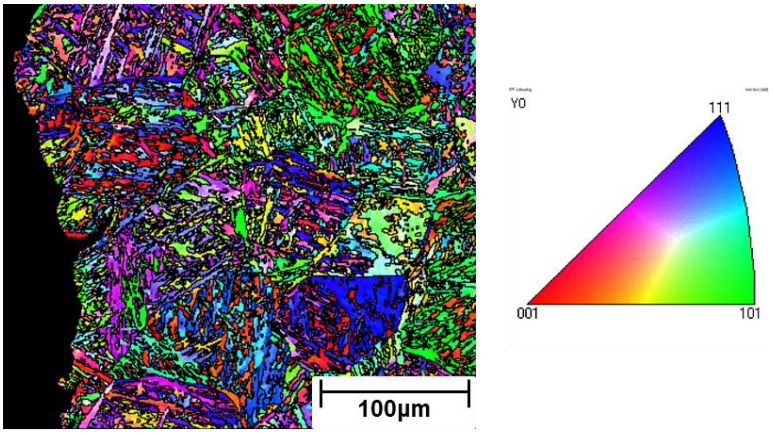

Figure 15: **EBSD-orientation map taken at the crack end (crack propagation direction) of the 5 Hz FCG test specimen (f = 5 Hz, T = 600 °C).**

4. Conclusion

The crack growth behavior of X20CrMoV12-1, a standard 12 % Cr ferritic/martensitic steel of the power industry was investigated concerning flexible power plant operation. Testing was performed in the temperature range from 300 °C to 600 °C in air. Testing frequency and holding times were especially considered. The following conclusions can be drawn from the experimental data and corresponding microstructural observation:

- With decreasing frequency (20 Hz → 5 Hz), the crack growth rate increases slightly in the entire temperature range from 300 °C to 600 °C.

- In comparison to FCG experiments at 5 Hz and 20 Hz larger crack propagation rates per cycle occur in the 300 s hold time experiments (effective frequency: 3.33×10^{-3} Hz) from 300 °C to 600 °C. It is noteworthy, that even at 300 °C and 400 °C larger crack growth increases per cycle occur in the 300 s hold time experiments in comparison to the FCG experiments carried out at 5 Hz and 20 Hz, although creep processes are of no relevance at such low temperature. A further increase of the hold time at 400 °C to 600 s (effective frequency: 8.33×10^{-4} Hz) did not lead to a further increase of the crack growth rate, what indicates that there is no influence of creep up to 400 °C.

- With holding times implemented into the testing cycle at maximum load significantly higher ΔK values are require in comparison to pure cyclic loading to start crack growth. This potentially poses further lifetime reserves if properly exploited, since very high stress intensities are needed for crack propagation.

- Up to 500 °C a dependency of crack growth rate on temperature was found for 300 s (effective frequency: 3.33×10^{-3} Hz) hold time experiments:

  - At temperatures of 550 °C the crack growth begins at significantly lower ΔK values.

  - At 600 °C crack growth is accelerated. The reasons for this are lower creep resistance and a superposition of dynamic recrystallization, starting from a critical ΔK value of ~ 32 MPa$\sqrt{m}$ and a crack growth rate of ~ 6.5×10^{-4} mm/Cycle.

- An increase in hold time to 600 s (effective frequency: 8.33×10^{-4} Hz) results in slightly larger crack propagation rates per cycle and to further increase of required ΔK values to start crack growth (temperature range from 500 °C to 550 °C). In contrast, increased hold time has no influence on crack growth at 400 °C. This indicates creep processes or creep fatigue interaction becoming significant from 500 ° C towards higher temperature.

- “Hook” formation in the da/dN vs. ΔK plots was observed in a less pronounced shape even at low temperature, where creep deformation does not play a role. Comparably high stress intensities required to start crack growth at low temperature are supposed to be a possible reason for this phenomenon. The phenomenon of the crack growth rate initially decreasing with increasing ΔK potentially poses further service life reserves if properly exploited in an advanced life time assessment code.

5. Outlook

This study evaluated the results of the holding time experiments according to the K-concept. In future work, the critical temperature / frequency / hold time- combination will be determined, from which the transition from fatigue-dominated crack growth to creep/fatigue interaction takes place. Moreover a suitable evaluation concept will be selected (e. g. J-Integral or C^*-Integral). For this purpose, comprehensive microstructure investigation will be carried out. Furthermore the influences of steam atmosphere on the start of crack growth and crack propagation behavior will be investigated in detail to provide all information necessary for improved exploitation of material inherent life time potentials in the future.

6. Acknowledgments

The authors gratefully acknowledge the German Federal Ministry for Economic Affairs and Energy for supporting this study under grant No. 03ET7024A. In addition, the authors would like to acknowledge the support of B. Werner, H. Reiners and D. Liebert in mechanical testing, V. Gutzeit and J. Bartsch in sample preparation and Dr. E. Wessel for performing the microstructural investigation.

References

[1] Eggeler G, Nilsvang N, Ilschner B. Microstructural changes in a 12% chromium steel during creep. Steel Res 1987;58–2:97–103.
[2] Maruyama K. Strengthening mechanisms of creep resistant tempered martensitic steel. ISIJ Int 2001;41:641–53.
[3] Petit J, Helnaff G, Sarrazin-Baudoux C. Environmentally-assisted fatigue in a gaseous atmosphere. Compreh Struct Integr 2003;6:211–80.
[4] Chen Q, Kawagoishi N, Nisitani H. Evaluation of fatigue crack growth rate and life prediction of Inconel 718 at room and elevated temperatures. Mater Sci Eng A 2000;277:250–7.
[5] Ennis PJ. A Czyrska-Filemonowicz: recent advanced in creep-resistant steels for power plant applications. Sādhanā India 2003;28(Parts 34):709–30.
[6] Makhlouf K, Jones JW. Effects of temperature and frequency on fatigue crack growth in 18% Cr ferritic stainless steel. Int J Fatigue 1993;15:163–71.
[7] Uematsu Y, Akita M, Nakajima M, Tokaji K. Effect of temperature on high cycle fatigue behavior in 18Cr–2Mo ferritic stainless steel. Int J Fatigue 2008;30:642–8.
[8] Ding J, Hall R, Byrne J. Effects of stress ratio and temperature on fatigue crack growth in a Ti–6Al–4V alloy. Int J Fatigue 2005;27:1551–8.
[9] Chen Q, Kawagoishi N, Nisitani H. Evaluation of fatigue crack growth rate and life prediction of Inconel 718 at room and elevated temperatures. Mater Sci Eng A 2000;277:250–7.
[10] Hossain N, Taheri F. Influence of elevated temperature and stress ratio on the fatigue response of AM60B magnesium alloy. J Mater Eng Perform 2011.
[11] Granacher J, Klenk A, Tramer M, Schellenberg G, Mueller F, Ewald J. Creep fatigue crack behavior of two power plant steels. Int J Press Vess Pip 2001;78:909–20.
[12] Lu YL, Chen LJ, Liaw PK, Wang GY, Brooks CR, Thompson SA, et al. Effects of temperature and hold time on creep-fatigue crack-growth behavior of HAYNES®230® alloy. Mater Sci Eng A 2006;429:1–10.
[13] Holdsworth S. Creep-fatigue interaction in power plant steels. Mater High Temp 2011;28:197–204.

[14] Mehmanparast A. Evaluation of the testing and analysis methods in ASTM E2760–10 Creep-fatigue crack growth testing standard for a range of steels; 2011. p.41–66.
[15] Narasimhachary SB, Saxena A. Crack growth behavior of 9Cr–1Mo (P91) steel under creep–fatigue conditions. Int J Fatigue 2013;56:106–13.
[16] Bassi F. Creep fatigue crack growth and fracture mechanisms of T/P91 power plant steel. Mater High Temp 2015;32:250–5.
[17] Ab Razak N, Davies CM, Nikbin KM. Creep-fatigue crack growth behaviour of P91 steels. Procedia Struct Integr 2016;2:855–62.
[18] Shi K. Crack growth behaviour of P92 steel under creep and creep-fatigue conditions. Mater High Temp 2014;31:343–7.
[19] Speicher M, Klenk A, Coleman K. Creep-fatigue interaction in P91 steel. In: Proceedings of 13th conference on fracture, June 16–21, 2013, Beijing, China; 2013.
[20] Saxena A. Creep and creep–fatigue crack growth. Int J Fract 2015;191:31–51.
[21] Nikbin K, Radon J. Prediction of fatigue interaction from static creep and high frequency fatigue crack growth data. London, SW7 2BX: Department of Mechanical Engineering, Imperial College; 1997.
[22] Gandy D. X20 CrMoV12-1 steel handbook. Palo Alto (USA): Electric Power Research Institute; 2006.
[23] VDTÜV Werkstoffblatt 110, Warmfester schweißgeeigneter Stahl, X20CrMoV11-1, Werkstoff-Nr. 1.4922, 03.2012.
[24] ASTM E647-08e1. Standard test methods for measurements of fatigue crack growth rates; 2008.
[25] Paris P, Erdogan F. A critical analysis of crack propagation laws. J Basic Eng Trans ASME 1963;85(4):528–33.
[26] Irwin GR. J Appl Mech 1957;24:S.361.
[27] Cherepanov GP. Crack propagation in continuous media: PMM vol. 31, no. 3, 1967, pp. 476–488. J Appl Math Mech 1967;31:503–12.
[28] Rice JR. A path independent integral and the approximate analysis of strain concentration by notches and cracks. J Appl Mech 1968;35:379–86.
[29] Landes JD, Begley JA. A fracture mechanics approach to creep crack growth. ASTM STP 590 1976:128–48.